Manuscript prepared for Atmos. Chem. Phys.
with version 2015/04/24 7.83 Copernicus papers of the LaTeX class copernicus.cls.
Date: 24 May 2016

New particle formation in the fresh flue gas plume from a coal-fired power plant: effect of flue gas cleaning

Fanni Mylläri[1], Eija Asmi[2], Tatu Anttila[1], Erkka Saukko[1], Ville Vakkari[2], Liisa Pirjola[3], Risto Hillamo[2], Tuomas Laurila[2], Anna Häyrinen[4], Jani Rautiainen[4], Heikki Lihavainen[2], Ewan O'Connor[2], Ville Niemelä[5], Jorma Keskinen[1], Miikka Dal Maso[1], and Topi Rönkkö[1]

[1]Department of Physics, Tampere University of Technology, P.O. Box 692, FI-33101 Tampere, Finland.
[2]Atmospheric Composition Research, Finnish Meteorological Institute, FI-00560, Helsinki, Finland.
[3]Department of Technology, Metropolia University of Applied Sciences, FI-00180, Helsinki, Finland.
[4]Helen Oy, FI-00090 Helen, Helsinki, Finland
[5]Dekati Ltd., Tykkitie 1, 36240 Kangasala, Finland

Correspondence to: Topi Rönkkö (topi.ronkko@tut.fi)

Abstract. Atmospheric emissions, including particle number and size distribution, of a 726 MW_{th} coal-fired power plant were studied experimentally from power plant stack and from flue gas plume dispersing in the atmosphere. Experiments were conducted under two different flue gas cleaning conditions. The results were utilised in a plume dispersion and dilution modelling taking into account particle formation precursor (H_2SO_4 resulted from the oxidation of emitted SO_2) and assessment related to nucleation rates. The experiments showed that the primary emissions of particles and SO_2 were effectively reduced by flue gas desulphurization and fabric filters, especially the emissions of particles smaller than 200 nm in diameter. Primary pollutant concentrations reached background levels in 200–300 seconds. However, the atmospheric measurements indicated that new particles larger than 2.5 nm are formed in the flue gas plume, even in the very early phases of atmospheric ageing. The effective number emission of nucleated particles were several orders of magnitude higher than the primary particle emission. Modelling studies indicate that regardless of continuing dilution of the flue gas, nucleation precursor (H_2SO_4 from SO_2 oxidation) concentrations remain relatively constant. In addition, results indicate that flue gas nucleation is more efficient than predicted by using atmospheric aerosol modelling. Especially, the observation of the new particle formation with rather low flue gas SO_2 concentrations changes the current understanding on the air quality effects of coal-combustion. The results can be used to evaluate the optimal ways to achieve better air quality particularly in polluted areas like India and China.

1 Introduction

In global scale, nearly 40 % of annual production of electricity is covered by coal combustion (EU, 2014). In addition to CO_2 emissions, known to have climatic effects, coal combustion causes emissions of other harmful pollutants like NO_x, SO_2, and particulate matter, all decreasing the air quality and increasing health related risks but also affecting climate directly and indirectly. For instance, SO_2 affect the climate indirectly because it tends to oxidize in atmosphere and form H_2SO_4, which affects particle formation. Coal combustion related air quality problems exist especially in developing countries like China (Huang et al., 2014) where the power production is not always equipped with efficient flue gas cleaning systems. However, with proper combustion and flue gas cleaning technologies the fine particle emissions of coal combustion can be decreased to very low level and also the emissions of gaseous pollutants other than CO_2 can be decreased (Helble, 2000; Saarnio et al., 2014). Particle mass and number emission factors for the 300 MW coal-fired power plant with electrostatic precipitator (ESP) and flue gas desulphurization unit (FGD) have been reported by Frey et al. (2014): the emission for particle mass (PM1) was 0.18 $\pm$ 0.06 mg MJ^{-1} and for fine particle number $2.3{\cdot}10^9 \pm 4.0{\cdot}10^9$ MJ^{-1}. However, it can be expected that particle emissions and also the characteristics, such as particle size, are highly dependent on technologies used in the power production. Only few studies have reported particle number size distributions and mean particle diameter for the coal combustion emissions. The mean particle diameters have been reported to be between 100 nm (Frey et al., 2014; Yi et al., 2008) and 1 μm (Yi et al., 2008; Lee et al., 2013). According to Saarnio et al. (2014), chemical composition of particles in the efficiently cleaned flue gas after the FGD is shifted towards desulphurization chemicals. Interestingly, sulphate particle emissions from coal combustion with proper cleaning technologies can restrain the global warming due to cooling effect of the particles (Frey et al., 2014; Charlson et al., 1992; Lelieveld et al., 1992).

Due to the emission limits of power plants, driven by needs for healthier environment, emissions should be kept at minimum. This can be achieved by different technologies. Flue gas NO_x emissions can be reduced in the power plant boiler by applying low-NO_x burners, whereas SO_2 emissions can be reduced by flue gas desulphurization (FGD) (Srivastava et al., 2001). Particle emissions can be reduced by electrostatic precipitators (ESP) and fabric filters (FF). Very low emission levels can be achieved by these techniques. For example from particle emission point of view, ESP typically removes 99% (Helble, 2000) of the fine particles. Further, Saarnio et al. (2014) showed that desulphurization plant with fabric filters remove up to 97 % of the fine particles. Combination of these techniques would then remove 99.97 % of the fine particle emissions of the particles formed in combustion. However, particle emission as well as the effects of technologies can differ from these if the emissions are measured from the diluted flue gas in the atmosphere. In principle, particle number and even particle mass can increase in the atmosphere for example due to the nucleation and condensation processes (Marris et al., 2012; Buonanno et al., 2012). However, there are very few observations of the processes in the diluting flue gas during the first few minutes after the stack.

Power plant plumes have been studied with aircrafts by measuring long distance cross-wind profiles of gases and particles (Stevens et al., 2012; Brock et al., 2002; Lonsdale et al., 2012; Junkermann et al., 2011). Stevens et al. (2012) and Lonsdale et al. (2012) have compared these measurements to modelling results, which were based on emission inventory values. Modelling results indicated that secondary particle formation occurs in the plumes after emission from the stack and the measurement results show correlation with the model especially at distances of 10-20 km. Brock et al. (2002) argue the secondary particle formation to begin at 2 hour aged plume. Study of Brock et al. (2002) has focused on plume ages 0 to 13 hours old power plant plumes. However, Brock et al. (2002) do not report particle number concentrations for fresh flue gas. Cross-wind profiles shown in the study of Stevens et al. (2012) were from 5 km to a bit over 50 km distances, and these results were also used in Lonsdale et al. (2012). On the contrary, Junkermann et al. (2011) followed the plume centre line based on the SO_2 concentrations and made also few cross-wind profiles of the studied plume.

The aim of this study was to characterize how the atmospheric emissions from a 726 MW coal-fired power plant depend on flue gas cleaning, i.e. desulphurization plant and fabric filters (later referred as "FGD+FF off" and "FGD+FF on"). In addition to the stack measurements for pollutants, the study aimed to show how the flue gas cleaning affects real atmospheric concentrations of emitted CO_2, SO_2 and particles. The study included experiments conducted in the stack of the power plant, measurements conducted with a helicopter equipped with instruments for CO_2, SO_2 and particles, and flue gas plume dispersion and aerosol process modelling.

2 Experimental

The studied power plant is a base-load station located near Helsinki city centre, Finland. The power plant consists of two 363 MW_{th} coal-fired boilers. The energy is produced by coal combustion in 12 low-NO_x technology burners (Tampella/Babcock-Hitachi HTNR low-NO_x), situating at the front wall of the boiler. The properties of coal used in this study are listed in SI1. Combustion releases flue gases that are cleaned in electrostatic precipitator (ESP), semi-dry desulphurization plant (FGD), and fabric filters (FF) before the stack. There are separate flue gas ducts and flue gas cleaning systems for each boiler.

The flue gas was studied in two different locations: the flue gas plume, and a reference point inside the stack. Measurements were made at both locations with two different flue gas cleaning situations: "FGD+FF off" and with all cleaning systems ("FGD+FF on"). The measurement location in the stack was at the height of +35 meters above sea level. The flue gas temperature inside the duct was 78 $\pm$ 2 °C in normal operation conditions and 130 $\pm$ 13 °C during "FGD+FF off" situation. The flue gas plume concentrations were measured with a helicopter equipped with aerosol instruments. The flying altitude of the helicopter was 150 meters above ground level or higher which corresponds to the LIDAR (Halo Photonics Streamline Doppler lidar with full-hemispheric scanning capability,

Pearson et al., 2009) (SI2) results for plume altitude. It should be noted that only the flue gases from the boiler under investigation were steered to bypass FGD and FF. Thus, in the "FGD+FF off" situation flue gas plume consisted of both the cleaned flue gas and the flue gas cleaned by ESP. This has to be kept in mind in the analysis of atmospheric measurements.

The measurements were made 24.3.2014 in two separate one hour periods (see specific times from SI2, the black rectangulars; the first illustrates "FGD+FF on" case and the latter "FGD+FF off" case). Weather conditions were stable during the study. The wind direction and speed were $216° \pm 5.51°$ (based on LIDAR data) and 6.5 m s^{-1} in "FGD+FF off" case and $220° \pm 6.25°$ and 4 m s^{-1} in "FGD+FF on" case, respectively. The marine boundary layer height was 246–258 meters and the planetary boundary layer heights were 360–530 meters. However the calculations were made within the marine boundary layer because the flue gas plume did not arise above it. The background aerosol concentrations for each measured gaseous component were: CO_2 403 ppm, SO_2 less than 2–8 ppb. The range of ambient temperature was 6.6–6.9 °C, the global radiation was 347–466 W m^{-2} and the visibility was 29043–36000 meters (see standard deviations from SI2) .

The instrument installations in different locations are shown in SI3. The sampling of flue gas in the stack was performed with Fine Particle Sampler (FPS; Dekati Ltd., Mikkanen et al., 2001) with total dilution ratio (DR) of 27. Probe and dilution air temperatures were at 200°C. The sample was led to instruments: Condensation Particle Counter (CPC3776; TSI Inc., Agarwal et al., 1980), ELPI (Dekati Ltd., Keskinen et al., 1992), SMPS (Wang and Flagan, 1990) 0.6/6 slpm (DMA3071, CPC3775 TSI Inc.) and gas analysers for diluted CO_2 (model VA 3100, Horiba) and NO, NO_2 and NO_x (model APNA 360, Horiba). Measurement data was also received from a normal operation monitoring of the emissions, including raw flue gas SO_2, NO_x, CO_2 concentrations and dust (SICK RM 230, calibrated based on SFS-EN 13284-1 standard). In contrast to stack sampling, the sample in the flue gas plume dilutes naturally and can be sampled to equipment without additional dilution of aerosol sample. The sampling inlet position in the helicopter is shown in SI3. Natural dilution causes rapid changes in concentrations and, thus, high measurement frequency equipment were used in the helicopter. CPC3776 (TSI Inc.) was installed to measure the total particle number concentration, whereas Engine Exhaust Particle Sizer (EEPS, TSI Inc., Mirme,1994) was measuring the particle number size distribution at 1 Hz sampling frequency from 5.6 nm to 560 nm. Gas concentrations for CO_2/CH_4/H_2O (Cavity spring-down spectrometry Picarro model G1301-m CO_2/CH_4/H_2O Flight Analyzer) and SO_2 (Thermo Scientific Inc. model 43i SO_2 analyzer, with 5 second response time) were measured continuously with 1 Hz frequency (see more details in SI7).

Fig. 1 shows the helicopter measurement routes for "FGD+FF on" and "FGD+FF off" situations. The objective of flight routes was to follow the centre line of the flue gas plume. Helicopter flew both up and down of the plume; the gps-data was used to separate these two flight situations to calculate the distance and the age of the plume separately.

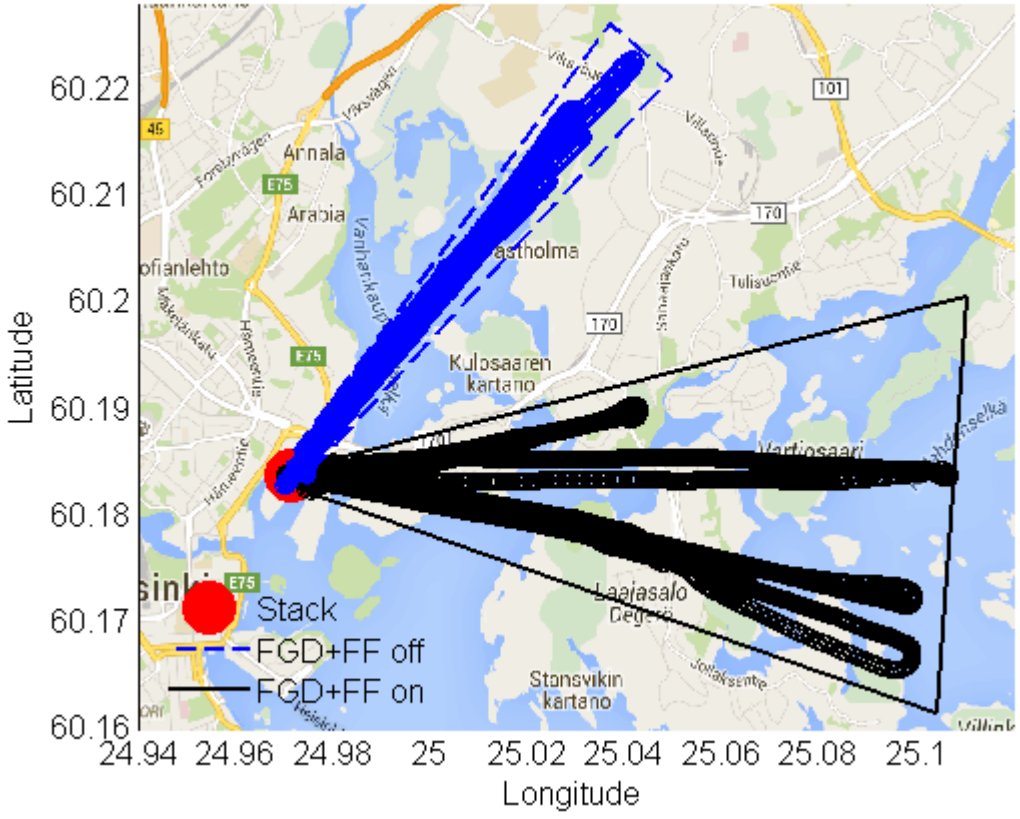

Figure 1. Helicopter flight routes. The wind blew in the angle of 216°± 5.51° (based on LIDAR data) and the flight direction was 213°±4.14° (based on GPS data for helicopter) in "FGD+FF off" (blue circles). Corresponding angles for "FGD+FF on" case (black circles) were 220°±6.25° (wind direction based on LIDAR data) and 223°±5.66° (flight direction based on GPS data for helicopter). The triangular shapes (black and blue lines) show the helicopter GPS coordinates that have been taken into account in the calculations.

2.1 Model description: Gaussian plume model

The Gaussian plume model is a solution to an advection-diffusion equation that describes the changes in the pollutant concentrations due to advection of wind and turbulent mixing with the surrounding air (Stockie, 2011). Accordingly, the concentration of a pollutant i, C_i, emitted from a point-like source, can be expressed as follows:

$$C_i(x,y,z) = \frac{Q_i}{2\pi U \sigma_y \sigma_z} \exp(-\frac{y^2}{\sigma_y^2})[\exp(-\frac{(z-H)^2}{\sigma_z^2}) + \exp(-\frac{(z+H)^2}{\sigma_z^2}] \quad (1)$$

Here x, y and z are the spatial coordinates, aligned so that x axis corresponds to the wind direction, and H is the height at which i is emitted (stack height). Also, Q_i is the emission rate of i at the source, U is the mean wind speed, and σ_z as well as σ_y are the so called dispersion coefficients which reflect

the spatial extent of the plume as a function of the downwind distance x. The dispersion coefficients were calculated using the parameterization of Klug (1969) and the atmospheric stability class, which is needed to calculate the dispersion coefficients. Atmospheric stability classes were estimated based on the measurements of the wind speed and solar radiative flux at the surface. Moreover, the pollutant concentrations were calculated along the centerline of the plume, the value of U was set to constant and equal to the average wind speed during the flights. Finally the value of z was set equal to the stack height (150 meters).

It is worth noting that the background concentration of i is zero according to eq. 1: $C_i \to 0$ when $z \to \infty$ or $y \to \pm\infty$ However, the flue gas emitted from the stack was actually cleaner, in terms of particle number concentration, than the background air when the flue gas was cleaned properly. In order to take into account for such cases, the following equation was used instead of eq. 1:

$$\hat{C} = C_\infty + \frac{C_0 - C_\infty}{C_0} \cdot C_i \tag{2}$$

where C_∞ is the background concentration of i, and C_0 is its concentration at the source. It can be readily shown that eq. 2 is a solution the advection-diffusion equation underlying eq. 1. Also, it is easily verified that $\hat{C} \to C_\infty$ when $z \to \infty$ or $y \to \pm\infty$. Finally, the value of Q_i in eq. 1 was chosen so that $\hat{C} \to C_0$ when $z \to H$ and x,$y \to 0$.

An important output of the model is the dilution ratio of the flue gas plume, DR, which is calculated based on equation 3.

$$DR(t) = \frac{[CO_2(t)] - [CO_{2,\infty}]}{[CO_{2,stack}] - [CO_{2,\infty}]} \tag{3}$$

In equation 3 [$CO_2(t)$] and [$CO_{2,\infty}$] are the modelled CO_2 concentration at time t and the CO_2 concentration measured in the stack, respectively.

2.1.1 Model description: Nucleation rate and particle formation calculations

The particle appearance (driven by nucleation and growth) rates for the particles 2.5 nm in diameter were calculated using the parameterization developed by Lehtinen et al. (2007) presented in eq. 4. The key input parameters for the model are the nucleation rate (J_{nuc}), the particle growth rate (GR), and the coagulation sink which describes the rate at which clusters are removed via coagulational scavenging ($CoagS$). The parameter J_{nuc} is calculated based on the estimated sulphuric acid concentrations as function of plume age as detailed below, and the particle growth rates are calculated by assuming growth only via irreversible condensation of sulphuric acid. Also, $CoagS$ is calculated from the condensation sink CS (which is calculated in a fashion described below) using the eq. 8 in Lehtinen et al. (2007). Also, the initial size of the freshly nucleated clusters was varied, and the value of the shape factor (m in Eq. 6 in Lehtinen et al. (2007)) was set equal to –1.6.

$$J_x = J_{nuc} \cdot \exp(-\gamma \cdot d_1 \cdot \frac{CoagS(d_1)}{CS}) \tag{4}$$

The nucleation rates J_{nuc} in the studied plume were calculated using the parameterization developed by Kulmala et al. (2006) which has also been applied previously to model nucleation in plumes (Stevens et al., 2012, 2013).

$$J_{nuc} = A \times [H_2SO_4] \tag{5}$$

In equation 5 A=1·10^{-7} s^{-1} or A=1·10^{-6} s^{-1} and [H_2SO_4] (cm^{-3}) is the sulphuric acid concentration. The value of A=1·10^{-7} s^{-1} was chosen according to the study of Stevens et al. (2012, 2013). The initial size size of the nucleated particles was assumed to be of 1.5 nm

Formation of [H_2SO_4] was calculated assuming that it is produced only via the OH + SO_2 reaction and the only loss pathway for H_2SO_4 is condensation onto the particle surfaces. When steady-state is assumed, the [H_2SO_4] can be calculated from equation 6.

$$[H_2SO_4] = k_1 \times \frac{[SO_2] \times [OH]}{CS} \tag{6}$$

In equation 6 k_1 is the reaction constant between OH and SO_2 (Table B.2 in Seinfeld and Pandis, 2008). The SO_2 concentrations were taken from the helicopter measurements, and the time development of CS and [OH] in the plume were modelled as follows. First, CS was calculated using the relation shown in equation 7.

$$CS = \frac{CS_{stack}}{DR} + CS_{\infty} \times (1 - \frac{1}{DR}) \tag{7}$$

In equation 7 CS_{stack} is the condensation sink of aerosols measured in the stack, and CS_{∞} is the condensation sink of the background aerosols. The value of the latter parameter was calculated from the size distributions measured at the SMEAR III station (Junninen et al., 2009) which is located around two kilometers away from the power plant. Second, [OH] was calculated using the parameterization of Stevens et al. (2012) which has downward shortwave radiative flux at the surface and [NO_x] as main inputs. Value for the former parameter was taken from the measurements (using the value averaged over the measurement periods), and the NO_x concentrations were calculated from equation 8.

$$[NO_x(t)] = \frac{[NO_{x,stack}]}{DR(t)} \tag{8}$$

In equation 8 [$NO_{x,stack}$] is the NO_x concentration measured in the stack. It should be noted here that in the calculations the background concentration of NO_x is assumed to be of minor importance when compared to NO_x emitted by power plant. To support this, the study of Pirjola et al. (2014) indicates that in the harbour area close to the power plant studied here the NO_x concentration level is typically clearly lower than 100 ppb.

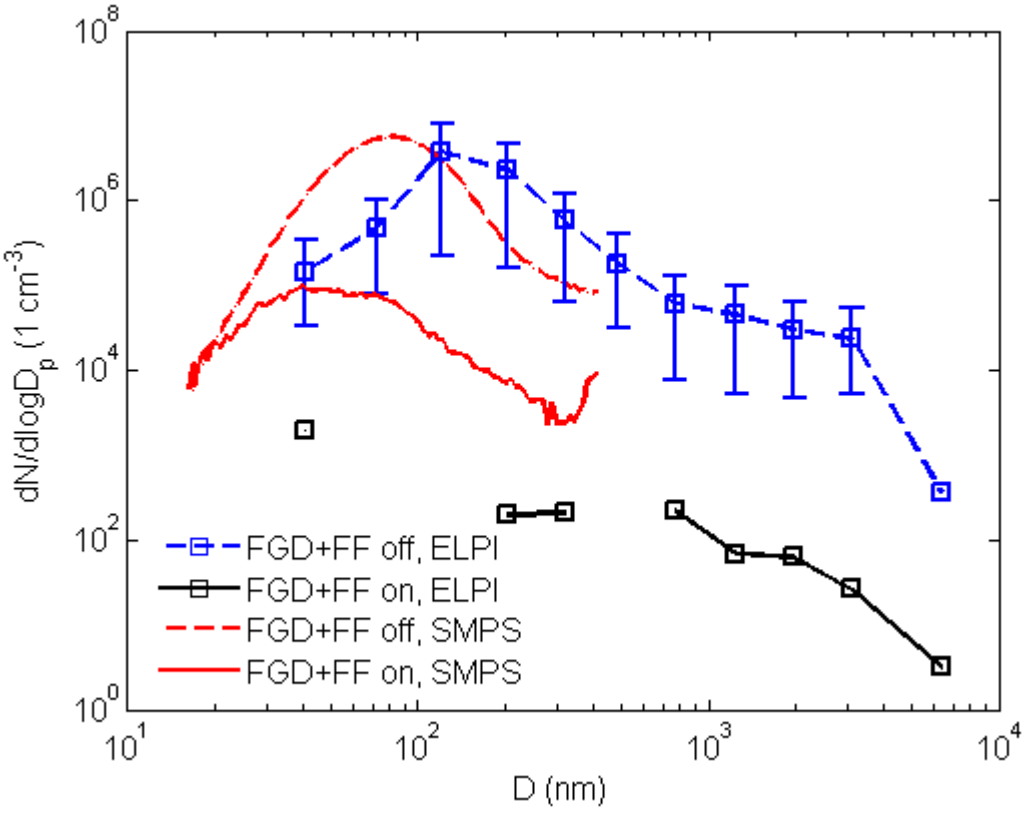

Figure 2. Particle size distributions measured with ELPI and SMPS from the flue gas in the stack. ELPI and SMPS data is shown in operation conditions, "FGD+FF on" and "FGD+FF off". The x-axis is aerodynamic diameter for ELPI data and electrical mobility diameter for SMPS data.

3 Results

3.1 Primary emissions of the coal-fired power plant

The SO_2 and particle emissions of the power plant were strongly dependent on flue gas cleaning system. This can be seen in Table 1 which shows flue gas concentrations for CO_2, SO_2, NO_x, O_2, particle number (N_{tot}), dust as well as flow rate in the duct in both flue gas cleaning conditions. In the shift from "FGD+FF off" to "FGD+FF on" situation the SO_2 concentration decreased nearly to fifth part, the concentration of dust decreased by a factor of 50 and the N_{tot} decreased by a factor of four thousand. For other parameters the effect of FGD+FF was insignificant.

Figure 2 shows the particle number size distributions of flue gas in the stack in both cleaning conditions. These were measured using an electrical low pressure impactor (ELPI) and a scanning mobility particle sizer (SMPS) in both "FGD+FF on/off" cases. In the "FGD+FF on" case the SMPS measurement is a median value over few hours of operation due to low particle number concentra-

Table 1. Flue gas concentrations of CO_2, SO_2, NO_x, O_2, total particle number (N_{tot}), dust, and flue gas flow rate in the stack. Mean values (+ standard deviation) are presented for both flue gas cleaning conditions ("FGD+FF on" and "FGD+FF off").

	FGD+FF off	FGD+FF on
CO_2 (%)	9.92 ± 2.2	10.3±0.96
SO_2 (ppbv)	243000±71300	55200±14600
NO_x (ppmv)	252±74	258±65
O_2 (%)	6.16±0.11	6.11±0.10
N_{tot} (cm^{-3})	$(1.8 \pm 0.2) \cdot 10^6$	420±640
Dust (mg/Nm^3)	188±82	4±1
Flow (Nm^3/h)	$(4.86 \pm 0.20) \cdot 10^5$	$(4.65 \pm 0.064) \cdot 10^5$

tions in the stack. Based on the SMPS measurement the particle geometric mean electrical mobility equivalent diameter was 80 nm and the width of particle number size distribution (geometric standard deviation, GSD) was 1.45 for "FGD+FF off" case. In comparison, the geometric mean electrical mobility equivalent diameter was 31 nm for "FGD+FF on" and the width of particle number size distribution was 2.15. Based on the measurements using the ELPI geometric mean aerodynamic equivalent diameter was 141 nm and GSD was 1.41. The difference in mean diameters measured using the ELPI and the SMPS comes from the differences in size classification principles of these instruments and enables the determination of effective density of measured particles. The effective density measurement and calculation is based on the relation between the electrical mobility equivalent diameter and the aerodynamic equivalent diameter of the particle (see Ristimäki et al. 2002). In this study case the difference in equivalent diameters indicates effective density larger than unit density for emitted particles (approximately 3.1 g cm^{-3}). In comparison, Saarnio et al. (2014) used effective density of 2.5 g cm^{-3} to convert the electrical mobility diameter measured using SMPS to aerodynamic diameter. When studying "FGD+FF on" case the particle concentrations were so low and thus accurate determination of mean particle size was not possible from the particle size distribution measured by the ELPI.

Flue gas sample from the stack was diluted with hot dilution air before the particle instruments and thus the particle number concentrations (Table 1) and particle size distributions (Figure 2) are for non-volatile particles. In combustion studies the hot dilution air is typically used to prevent the formation of liquid nucleation particles and to minimize the effects of condensation of semi-volatile compounds on particles. However, to ensure the measured particles were non-volatile and not affected by the dilution method itself, a thermodenuder (Rönkkö et al., 2011) was used periodically after the sampling and dilution. The thermodenuder did not affect the particle number size distribution, which confirms the non-volatile nature of the measured particles. Due to this non-volatility of

the particles, the life time of the primarily emitted particles in the atmosphere can be longer than that of volatile particles, e.g. nucleation mode particles observed in vehicle exhaust (Lähde et al., 2009).

3.2 Atmospheric measurements

Figure 3 shows the measured flue gas plume concentrations as a function of plume age. Diffusion losses for the particles in the sampling lines were calculated based on the measurement setup. The data was recorded based on gps-coordinates which were used to calculate distances from the stack, and the distances were changed to correspond plume age using wind speeds 6.5 m s^{-1} and 4.0 m s^{-1} (LIDAR, S3). The calculation showed that nearly 70% of the 2.5 nm particles in diameter was lost in the sampling lines and thus the total concentration shown in Figure 3 can be higher than shown here. The vertical lines denote the 2 km distance from the stack. Figure 3 shows the dilution time scale of the flue gas in terms of CO_2 and SO_2 in both operation conditions. Same trend in SO_2 and N_{tot} concentrations as observed in Table 1, was measured by instruments installed in the helicopter; in "FGD+FF off" situation the particle and SO_2 concentrations were higher than the "FGD+FF on" situation. It should be kept in mind that in "FGD+FF off" situation only one of the two flue gas cleaning systems was bypassed.

Plume dilution can be evaluated by the CO_2 concentrations (in Figure 3 a and b), which show that the "FGD+FF off" case dilutes to approximately background level in 200 seconds (0.74 km) and the "FGD+FF on" case in 300 seconds (1.5 km). The peak values for CO_2, SO_2 and N_{tot} were 3195 ppm, 2193 ppb, $3.\cdot10^4$ cm^{-3} in the "FGD+FF off" situation and 3254 ppm, 585 ppb, $0.4\cdot10^4$ cm^{-3}, respectively, for the "FGD+FF on". However, the dilution decreases the CO_2, SO_2 and N_{tot} concentrations in the atmosphere to 422 ppm, 52 ppb in "FGD+FF off" situation, and 473 ppm, 89 ppb in "FGD+FF on" situation. Respectively, the N_{tot} reached nearly background concentrations after 200 seconds and 300 seconds. The background gaseous concentrations for each measured gaseous component were 403 ppm and 2-8 ppb, for CO_2 and SO_2 respectively. The boundary layer mixing started during the "FGD+FF on" measurements and thus the background values measured from the upwind side flight loops from the stack were averaged and subtracted from both "FGD+FF on/off cases". It can be noted that very near (first 10–50 seconds) the stack the helicopter was not in the plume. This can be seen from CO_2 and SO_2 concentration values presented in Figure 3a and 3b when approaching plume age zero. Thus, the dilution process is discussed below, mainly, from the maximum concentrations forward.

An increase in total particle concentration can be seen in Figure 3 after 400 seconds aged the flue gas plume. This tendency can be seen in both flue gas cleaning situations. Based on Figure 3a, for "FGD+FF off" case the background particle concentration was 1430 cm^{-3}, after 200 seconds the concentration was at the background level and after 400 seconds it increased significantly, even up to average level of 5 000 cm^{-3}. Based on CO_2 measurements, the dilution of flue gas was practically complete at 200 seconds. Similarly, in "FGD+FF on" case after 500 seconds the particle concen-

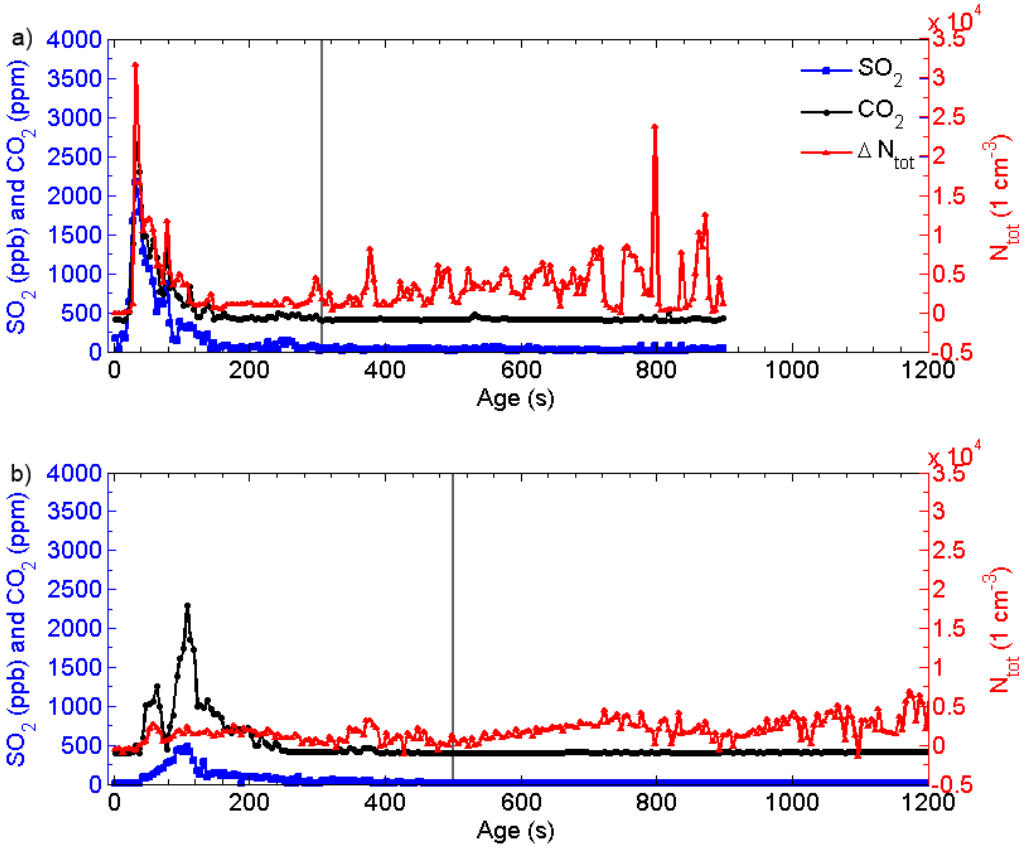

Figure 3. Concentrations of power plant flue gas components measured by instrument installed in to the helicopter as a function of plume age; "FGD+FF off" on the left and "FGD+FF on" on the right. SO_2 (ppb, blue line) and CO_2 (ppm, black line) concentrations on the left axes and total particle number concentration ΔN_{tot} (1 cm^{-3}, red line, from CPC) on the right axes. The ΔN_{tot} is calculated using the background value calculated upwind side of the stack ($CO_{2,bg}$ was 403 ppm and $SO_{2,bg}$ 2-8 ppb). The grey vertical lines denote 2 km distance from the stack in "FGD+FF on/off" cases. The presented results are 5 second median values.

tration was slightly above background, after which increasing even up to 5 000 cm^{-3} after 700 seconds. Thus, the concentrations in the diluted and aged flue gas plume were higher than the background and significantly higher than could be expected based on the primary particle concentrations and observed dilution profiles. In general, taking into account the fact that there is no comprehensive measurement of the primary precursor matrix (only [SO_2] is measured), the primary precursor matrix might include low-volatile organics and SO_3 which can increase the probability of new particle formation. Due to the increasing trend in particle concentration, some estimation about formation rates can be calculated. Depending on the plume age the mean formation rates calculated from the data shown in Figure 3 depended on the plume age being for "FGD+FF off" case 0–81 cm^{-3} s^{-1} and for "FGD+FF on" case 0 cm^{-3} s^{-1} to 18 cm^{-3} s^{-1} (mean slope of increasing total particle number concentration at 400–482 s and 500–692 s).

Particle size distributions, shown in SI5, were calculated from the EEPS data measured from the helicopter in both "FGD+FF on/off" situations as 10 second moving median method. The particle size distribution in the "FGD+FF off" case had a mode around 80 nm, which refers to the solid particle median diameter measured with the SMPS from the flue gas in the stack. The particle size distribution measurement made by using the EEPS (SI5) supports the results for total particle number measurement made by the CPC (Figure 3), i.e. in terms of particles the flue gas is diluting in 0–300 seconds in "FGD+FF off". In addition, the particle size distributions measured by the EEPS indicates slight increase of nanoparticle concentrations during the dilution and dispersion of the flue gas in the atmosphere. Although, EEPS total particle number concentration cannot be compared to total concentration of CPC because Levin et al. (2015) showed that EEPS total particle number concentration is not comparable with a CPC. Further, the Figure in SI5 the EEPS particle size distribution data is noisy and based on Awasthi et al. (2013) can show maximum of 67 % wrong compared to SMPS.

3.3 Model Calculations: Modelled vs measured CO_2 concentrations

The validity of the Gaussian plume model was tested against CO_2 measurements from the plume. Median CO_2 concentrations were calculated using the measurement data at a five seconds interval separately for the "FGD+FF on/off" cases, and the locations of the peak CO_2 concentration (tmax, [$CO_{2,max}$]) were identified from the resulting time series. The value C_0 was chosen to eq. 2 so that the modelled CO_2 concentration, $\hat{C}_{CO2}$, was around [$CO_{2,max}$] when $t = t_{max}$. The choice of C_0 was made in this manner rather than initializing the model to use the stack concentrations due to the following two reasons. First, Gaussian plume model does not yield reliable results close, i.e. within a few tens of meters, to the source (Arya, 1995). Second, the comparison of the results near (first 10–50 seconds) the source is problematic because the helicopter was not located at the plume centerline during the initial stages of the measurements.

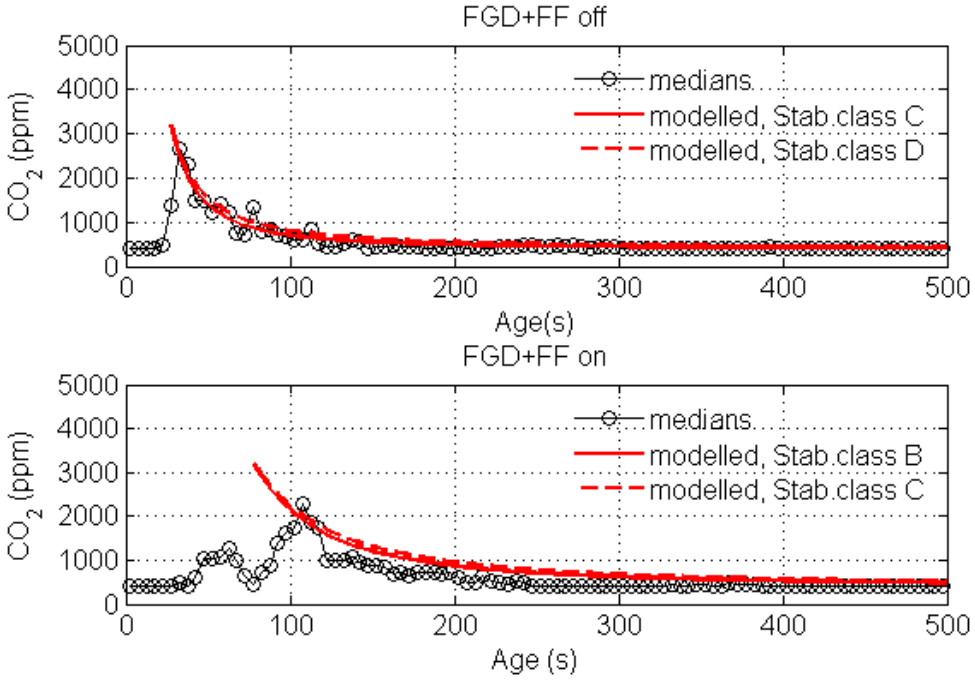

Figure 4. Comparison of measured and modelled CO_2 concentrations. Median of measured values are shown with black (circle) symbols along with the standard deviations. Dashed and dotted red lines correspond to model results for stability classes 'b' and 'c' (top panel) and 'c' and 'd' (bottom panel), respectively. The correlation coefficients between the model and the measurements are shown in Table 2

Comparison of the measured and modelled CO_2 concentrations is shown in Figure 5 and in Table 2. The chosen stability classes were 'b' and 'c' as well as 'c' and 'd' for the "FGD+FF on" and "FGD+FF off" cases, respectively, corresponding to the stability conditions ranging from unstable to neutral (Pasquill, 1961). As can be seen, the model reproduces the observed trends rather well, in particular for the "FGD+FF off" case, while the model tends to slightly overestimate the observed concentrations for the "FGD+FF on" case. The modelled and measured concentrations were within one standard deviation in general. Mean relative error (MRE) and correlation coefficients (R^2) were calculated between the measured and modelled concentrations for CO_2. In order to further investigate the performance of the model, comparison was made between measured SO_2 and Gaussian model diluted SO_2 concentrations, shown in SI6. The results showed that the model consistently overestimates the SO_2 concentration in the plume, typically by a factor between 3 and 4, compared to the measured values. This difference could be partly explained by the oxidation of SO_2 because it is not taken into account by the model. However, this discrepancy between MRE's and R^2 does not affect the model performance as the measured SO_2 concentrations, instead of modelled, were used in the plume model simulations.

Table 2. Comparison between modelled CO_2 concentration and measured CO_2 concentration, and comparison between SO_2 measured from the atmosphere and Gaussian model diluted SO_2. Mean relative error (MRE) and correlation coefficients (R^2) were calculated between measured and modelled concentrations.

		CO_2		SO_2	
case	stab.class	MRE (%)	R^2	MRE (%)	R^2
"FGD+FF off"	c	5	0.97	131	0.95
	d	25	0.97	322	0.96
"FGD+FF on"	b	29	0.87	291	0.84
	c	40	0.87	413	0.85

3.4 Model Calculations: Nucleation and new particle formation

Modelled and measured CO_2 concentrations showed that the model reproduced the observed dispersion of the plume relatively accurately. Thus the model was applied to calculate [NO_x], [OH], and [H_2SO_4] which were needed to investigate possibility of new particle formation in the plume. These results are summarised in Figure 6. It is seen that sulphuric acid concentrations exponentially increase during the initial stages of the simulation and then reach constant concentration around $1{\cdot}10^6$ and $1{\cdot}10^7$ cm^{-3}, a range which is comparable also with the atmospheric observations of [H_2SO_4] (Mikkonen et al., 2011) formation. Mikkonen et al., (2011), have reported that H_2SO_4 concentrations varied between $1.86{\cdot}10^5$ – $2.94{\cdot}10^6$ molec cm^{-3}, and Sarnela et al., (2015) reported [H_2SO_4] concentrations $4.4{\cdot}10^6$–$11.5{\cdot}10^6$ molec cm^{-3} for Finnish industrial and non-industrial area. More H_2SO_4 is formed in the "FGD+FF off" case because of higher primary SO_2 emission compared to the "FGD+FF on" case.

Initially, OH concentrations are lowered by large concentrations of NO_x which subsequently decreases during plume ageing. NO_x reduction leads to increases in [OH] and [H_2SO_4]. While the [OH] increased consistently during the simulations, [SO_2] decreased because of dilution. Due to these opposed trends, the production term for the sulphuric acid, in equation 6, did not change greatly during the later stages of the simulations. Moreover, the condensation sink (CS) diluted rapidly to its background value, which was around $1{\cdot}10^{-2}$ s^{-1}. These facts explain why the modelled sulphuric acid concentrations, calculated with equation 6, did not change notably after the initial, rapid increase.

The modelled nucleation rate J_{nuc} is directly proportional to the sulphuric acid concentration and hence the trends in [H_2SO_4] are directly reflected in J_{nuc} (Figure 6). Furthermore, in our measurements the particles were detected at the lowest CPC detection limit which was 2.5 nm, $J_{2.5}$. According to the scheme applied here (see equations 4 and 5), the fraction of freshly nucleated particles that survive into detectable sizes depends mainly on their growth rate (GR) and on the condensation sink (CS). The average given by the model GRs were 0.34 or 0.19 nm/h in the "FGD+FF off" case, and 0.07 or 0.04 nm/h in the "FGD+FF on" case for the two stability class scenarios. These values are

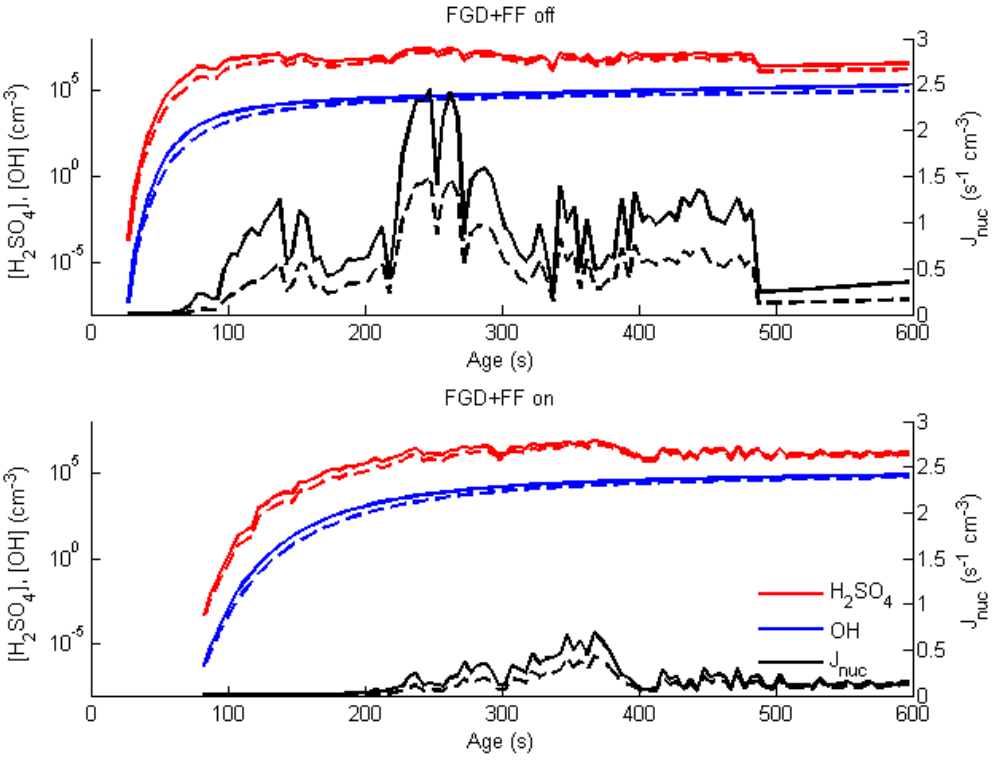

Figure 5. Time development of [H_2SO_4] (red lines), nucleation rate (black lines), [OH] (blue lines) (cm^{-3}). Dashed and dotted red lines correspond to model results for stability classes 'c' and 'd' (top panel) and 'b' and 'c' (bottom panel), respectively.

clearly smaller than atmospheric GR observations in urban areas (e.g. Stoltzenburg et al., 2005). As a lower GR leads to a lower surviving fraction, we conclude that the modelling results do not explain the observed particle formation in the flue gas plume.

A series of additional calculations were performed in order to investigate the sensitivity of the results to the values of the key input parameters. First, J_{nuc} is proportional to the constant A whose exact value is not accurately known, and this uncertainly translates directly into the calculated nucleation rates. A sensitivity analysis was made for the nucleation model in order to evaluate the sensitivity of nucleation rates to the value of A (shown in Table 3). In these calculations, a value of $1{\cdot}10^{-6}$ was chosen for A which is an order of magnitude higher than in base case simulations. The choice of the value was based on the study of Sihto et al. (2006) who investigated NPF events occurring on boreal forest. As can be seen, increased value of A is not sufficient alone to explain observed new particle formation. A second source of uncertainty is terms of the sulfuric acid concentration which was calculated using a rather simple scheme (see section 2.1.1). Increases in [H_2SO_4] leads to both increased J_{nuc} and GR and ultimately to larger $J_{2.5}$. Results displayed in Table 3 show

that $J_{2.5}$ is more consistent with observations when $[H_2SO_4]$ is increased five or ten-fold and when A is set equal to $1{\cdot}10^{-6}$ like in Sihto et al. (2006). Therefore, underestimation of $[H_2SO_4]$ may explain the discrepancy between the obeservations and base case model results. This might caused by underestimation of [OH] or overestimation of CS. Regarding the modeled OH concentrations, it can be noted that they are relative low, reaching values of around $1{\cdot}10^5$ cm^{-3} by the end of the flights. In comparison, concentrations of around $1{\cdot}10^6$ cm^{-3} have been reported during the daytime around noon in various atmospheric environments (Hofzumahaus et al., 2009; Petäjä et al., 2009), $0.26{\cdot}10^6$ molec cm^{-3} in Mace Head (Berresheim et al., 2002), and $1{\cdot}10^6$–$2{\cdot}10^7$ molec cm^{-3} in Atlanta (Kuang et al., 2008). Relative low modeled OH concentrations can be explained by high NO_x concentrations which were calculated to decrease consistely from several tens of ppm down to around 200 ppb during the flights (not illustrated here). Such high concentrations of NO_x are consistent with low [OH] (see Figure 1 in Lonsdale et al., 2014). It could be thus speculated that model underestimates $[H_2SO_4]$, and consequently rate of new particle formation, due to overestimation of $[NO_x]$. Moreover, it should be noted that neither SO_3 nor low-volatile organic vapours that might have been present in the measured flue gas were not accounted for in the modeling study. Previous studies suggest that these exhaust compounds may increase also the formation rate of nucleation particles (Pirjola et al., 2015; Ehn et al., 2012; Arnold et al., 2012) which may also explain the discrepancy between measurements and model calculations. Regarding the estimation of the value of CS, it should be noted that its values were taken from the field site measurements located nearby rather than from in-situ measurements. Therefore it can be speculated that actual CS values were lower than those used as input to the model which cause additional uncertainties.

3.5 Discussion

Each power plant (over 50 MW) in EU has emission limits for SO_2, NO_2, and particle mass concentrations, for the studied power plant the limits are 600 mg Nm^{-3} (210 ppm), 600 mg Nm^{-3} (290 ppm), and 50 mg Nm^{-3}, respectively. Comparison of the results in Table 1 with these emission limits shows that the emissions were clearly below these limits when the power plant operation was normal ("FGD+FF on"). It was observed that these low emissions can be achieved by properly working flue gas cleaning systems. In addition to primary emissions, flue gas cleaning systems seemingly affect also the compounds which can act as precursors for new particles; e. g. SO_2 tends to oxidize in the atmosphere to SO_3 and, further, to form H_2SO_4 which can nucleate or condensate to particle phase. This study shows clearly the importance of flue gas cleaning technologies, and underlines the proper usage of the technologies when the atmospheric pollution is discussed in terms of coal combustion. E.g. according to Huang et al. (2014) in Xi'an and Beijing 37% of sulphate in the atmospheric particles is emitted from coal burning.

In this study the power plant plume diluted to background levels in 2 km (200–400 seconds) which is faster than in other in-flight measurements (Stevens et al., 2012; Junkermann et al., 2011). This

Table 3. Sensitivity analysis made for number of particles formed with diameters above 2.5 nm during the flight (1 cm^{-3} s^{-1}) in the atmosphere with different values of A and $[H_2SO_4]$. The $[H_2SO_4]$ is calculated based on the measurement results and scaled up to test faster nucleation rate for both "FGD+FF on" and "FGD+FF off" cases and stability classes (sc).

		A=1 · 10^{-7} s^{-1}					
	sc	1·$[H_2SO_4]$	1.25·$[H_2SO_4]$	1.5·$[H_2SO_4]$	2·$[H_2SO_4]$	5·$[H_2SO_4]$	10·$[H_2SO_4]$
"FGD+FF off"	b	$1.00 \cdot 10^{-4}$	$5.36 \cdot 10^{-4}$	$1.73 \cdot 10^{-3}$	$8.29 \cdot 10^{-3}$	0.289	1.74
	c	0	0	0	$4.32 \cdot 10^{-4}$	$4.78 \cdot 10^{-2}$	0.44
"FGD+FF on"	c	0	0	0	0	$4.27 \cdot 10^{-4}$	$1.85 \cdot 10^{-2}$
	d	0	0	0	0	0	$1.73 \cdot 10^{-3}$
		A=1 · 10^{-6} s^{-1}					
	sc	1·$[H_2SO_4]$	1.25·$[H_2SO_4]$	1.5·$[H_2SO_4]$	2·$[H_2SO_4]$	5·$[H_2SO_4]$	10·$[H_2SO_4]$
"FGD+FF off"	b	$1.00 \cdot 10^{-3}$	$5.36 \cdot 10^{-3}$	$1.73 \cdot 10^{-2}$	$8.29 \cdot 10^{-2}$	2.89	17.4
	c	0	0	$4.47 \cdot 10^{-4}$	$4.32 \cdot 10^{-3}$	0.48	4.43
"FGD+FF on"	c	0	0	0	0	$4.27 \cdot 10^{-3}$	0.19
	d	0	0	0	0	0	0.017

difference may be because the dilution of plume and other processes are affected by source strength, background concentrations, and meteorology (Stevens et al., 2012). We observed that while SO_2 and CO_2 were already diluted to background levels the effect of the source to aerosol concentration was still clearly distinguishable after 2 km. In our study, we collected high-time-resolution data close to the power plant stack, which enable us to model the plume dilution on a detailed scale. From this, we were able to observe that while SO_2 and CO_2 were already diluted to background levels at a distance of 2 km – in agreement with the dilution modeling – the effect of the source to the aerosol number concentration was distinguished at distances >2 km. We attribute this to nucleation taking place in the ageing plume.

According to modelling results of Stevens et al. (2012), atmospheric new particle formation via coal combustion originated sulphuric acid nucleation begins at 1 km distance from the source whereas the sulphuric acid formation begins right after emission. Our study therefore supports this previous modelling work by showing that nucleation may take place in the aged plume and being the most effective after 400 seconds, corresponding approximately 2 km distance from the emission source in atmosphere.

In the light of the new results authors would like to distinguish the primary particle emission from the newly formed particle emission because those particles have different effects on the atmosphere and different formation mechanisms. Comparing primary particle emission with newly formed particle emission, the effects of different particles in the atmosphere could be taken into account more precisely in aerosol models or air quality assessment.

For instance, rough estimates for particle number emission factors can be calculated by comparing the measured particle number concentration with the simultaneously measured CO_2 concentration of the flue gas plume (see e.g. Saari et al. 2016). By utilizing this method, for particles existing in the flue gas plume in ages of 25–55 seconds the emission factor in respect of CO_2 was $2.0 \cdot 10^{10}$ (g $CO_2)^{-1}$ and in ages over 400 seconds $8 \cdot 10^{10}$ (g $CO_2)^{-1}$ in the "FGD+FF off" case. Similarly, in the "FGD+FF on" case the emission factors were $4 \cdot 10^{9}$ (g $CO_2)^{-1}$ (for aerosol dispersed 55–85 seconds in the atmosphere) and $3.74 \cdot 10^{10}$ (g $CO_2)^{-1}$ (for aerosol dispersed more than 500 seconds in the atmosphere). In comparison, the primary emissions were $1.75 \cdot 10^{10}$ (g $CO_2)^{-1}$ for "FGD+FF off" case and $8.0 \cdot 10^{6}$ (g $CO_2)^{-1}$ for "FGD+FF on" case. Thus, new particle formation can increase the real atmospheric particle number emissions even several orders of magnitude. It should be noted that the particle formation depends strongly on the plume age, [SO_2] and primary particle concentrations, and it is possible that there are some low-volatile organics or SO_3 present at the plume affecting the nucleation.

Our observations show that the number of secondary particle formed in the flue gas plume can be several orders of magnitude higher than the primary particles directly emitted from the flue gas duct. The formation can be observed already at a distance of ca 2 km from the stack; this distance is significantly lower than the grid size used in many atmospheric models, which demonstrates the need for subgrid parameterizations for power plat-originated secondary particles. Such a parameterization does already exist (Stevens et al., 2013), but it does not account for different types of sulphur removal technologies such as semi-dry desulphurization, wet desulphurization. Determining the effect of different removal technologies on power plant secondary aerosol production would increase the accuracy of particle loading predictions for regional air quality and global models.

4 Conclusions

Emissions of a coal-fired power plant into the atmosphere were studied comprehensively, for the first time, by combining direct atmospheric measurements, measurements conducted in the power plant stack, and modelling studies for atmospheric processes of flue gas plume. The stack measurements were made to estimate the effectiveness of flue gas cleaning technologies, such as filtering and desulphurization. It was shown that the flue gas cleaning technologies had a great effect on the SO_2 and total particle number concentrations in the primary emission. SO_2 concentration was reduced to fifth of "FGD+FF off" situation compared to "FGD+FF on" situation and the total non-volatile particle number concentration was reduced by orders of magnitude. Similar trend in primary emission reduction was detected in the atmospheric measurements. In addition, the reduction in primary emissions affects directly the concentrations of gaseous precursors (SO_2) for secondary particle formation in the atmosphere.

It was observed that the flue gas dilutes to background concentrations in 200–300 seconds. This dilution time scale is faster than reported in previous studies. However, the concentration profiles also showed an increase in particle number concentration in an aged flue gas, dilution and dispersion processes. To validate the dilution time scale, a Gaussian model was used to calculate the dilution in the atmosphere taking into account the primary emission and weather conditions. The Gaussian model confirms the dilution time scale, and the dilution ratio could be used to calculate the theoretical maximum values for different components in the flue gas plume. Weather conditions and theoretical maximum value for [NO_x] was used to calculate the [OH] formation rate and further [H_2SO_4] formation rate. These were calculated because the measurement results showed an increase in particle number concentrations in the flue gas plume during the dilution process. The modelling results for [H_2SO_4] formation rate support the hypothesis of sulphuric acid formation, but the sulphuric acid formation itself does not totally explain the increase in the total particle number concentration, therefore, e.g. low-volatile organics may excist on the flue gas plume. The sensitivity analysis of the [H_2SO_4] formation showed that the atmospheric parametrization is not enough to explain the processes in the flue gas plume.

Comparison between the primary particles and newly formed particles show that in the flue gas plume of coal-fired power plant the concentration of newly formed atmospheric particles can be several orders of magnitude higher than the primary particles from the flue gas duct; therefore, they should be considered when discussing emissions of power production. Including the effect of varying flue gas cleaning technologies in parameterizations of power-plant-originated secondary particles is a necessary step in understanding their importance.

Acknowledgements. The study was conducted in the MMEA WP 4.5.2. of Cleen Ltd., funded by Tekes (the Finnish Funding Agency for Technology and Innovation). Authors like to acknowledge B.Sc. Anna Kuusala and Mr Joni Heikkilä for programming Matlab, Mr Aleksi Malinen for measurement help. F.M. acknowledges TUT Graduate School, KAUTE-foundation, TES-foundation for financial support. E.A. and E.O. acknowledge the support of the Academy of Finland Centre of Excellence program (project number 272041). V.V. acknowledges the financial support of the Nessling foundation (grant 201500326) and the Academy of Finland Finnish Center of Excellence program (grant 1118615). F.M. and T.R. acknowledges the financial support from the Academy of Finland ELTRAN (grant 293437).

References

Agarwal, J. K., Sem, G. J. Continuous Flow, Single-particle Counting Condensation Nucleus Counter. Journal of Aerosol Science, 1980, (11), 343–357.

Arnold, F., Pirjola, L., Rönkkö, T., Reichl, U., Schlager, H., Lähde, T., Heikkilä, J., Keskinen, J. (2012) First online measurements of sulfuric acid gas in modern heavy-duty diesel engine exhaust: Implications for nanoparticle formation. Environmental Science and Technology, 46 (20), pp. 11227–11234.

S. P. Arya, Modeling and parameterization of near-source diffusion in weak winds. J. Appl. Meteorol. 1995, 34, 1112-1122.

A. Awasthi, B.-S. Wu, C.-N. Liu, C.-W. Chen, S.-N. Uang and C.-J. Tsai. The effect of nanoparticle morphology on the measurement accuracy of mobility particle sizers. MAPAN-Journal of Metrology Society of India, 2013, 28(3), 205-215.

H. Berresheim, T. Elste, H. G. Tremmel, A. G. Allen, H.-C. Hansson, K. Rosman, M. Dal Maso, J. M. Mäkelä, M. Kulmala. 2002. Gas-Aerosol relationships of H_2SO_4, MSA, and OH: Observations in the coastal marine boundary layer at Mace Head, Ireland. Journal of Geophysical Research, vol 107, no. D19, 8100, doi:10.1029/2000JD000229

C.A. Brock, R.A. Washenfelder, M. Trainer, T.B. Ryerson, J.C. Wilson, J.M. Reeves, L.G. Huey, J. S. Holloway, D.D. Parrish, G. Hübler, F.C. Fehsenfeld. (2002) Particle growth in the plumes of coal-fired power plants. Journal of Geophysical Research, 2002, 107:D12, 4155.

G. Buonanno, P. Anastasi, F. DiIorio, A. Viola. Ultrafine particle apportionment and exposure assessment in respect of linear and point sources, Atmospheric Pollution Research, 2012, 1, 36-43.

R. J. Charlson, S. E. Schwartz, J. M. Hales, R. D. Cess, J. A. Coakley, Jr., J. E. Hansen and D. J. Hofmann. Climate Forcing by Anthropogenic Aerosols. Science New Series, 1992, Vol. 255, No. 5043, 423-430

Ehn, M., Kleist, E., Junninen, H., Petäjä, T., Lönn, G., Schobesberger, S., Dal Maso, M., Trimborn, A., Kulmala, M., Worsnop, D.R., Wahner, A., Wildt, J., Mentel, T.F. (2012) Gas phase formation of extremely oxidized pinene reaction products in chamber and ambient air. Atmospheric Chemistry and Physics, 12 (11), pp. 5113–5127.

EU, The EU Emissions Trading System (EU ETS), http://ec.europa.eu/clima/policies/ets/index_en.htm (accessed 15.12.2014)

A. K. Frey, K. Saarnio, H. Lamberg, F. Mylläri, P. Karjalainen, K. Teinilä, S. Carbone, J. Tissari, V. Niemelä, A. Häyrinen, J. Rautiainen, J. Kytömäki, P. Artaxo, A. Virkkula, L. Pirjola, T. Rönkkö, J. Keskinen, J. Jokiniemi, R. Hillamo. Optical and Chemical Characterization if Aerosols Emitted from Coal, Heavy and Light Fuel Oil, and Small-Scale Wood Combustion, Environmental Science & Technology, 2014, 48, 827-836.

J.J. Helble. A model for the air emissions of trace metallic elements from coal combustors equipped with electrostatic precipitators, Fuel Processing Technology, 2000, 63, 125-147.

R.-J. Huang, Y. Zhang, C. Bozzetti, K.-F. Ho, J.-J. Cao, Y. Han, K. R. Daellenbach, J. G. Slowik, S.M.Platt, F. Ganonaco, P. Zotter, R. Wolf, S. M. Pieber, E. A. Bruns, M. Grippa, G. Ciarelli, A. Piazzalunga, M. Schwikowsko, G. Abbaszade, J. Schnelle-Kreis, R. Zimmerman, Z. An, S. Szidat, U. Baltenspergerm I. El Haddad, A. S. H. Pr*évô*t. High secondary aerosol contribution to particulate pollution during haze event in China, Nature, 2014, 514, 218-222.

Hofzumahaus, A., F. Rohrer, K. Lu, B. Bohn, T. Brauers, C.-C. Chang, H. Fuchs, F. Holland, K. Kita and Y. Kondo (2009). Amplified trace gas removal in the troposphere. Science 324(5935): 1702-1704

W. Junkermann, R. Hagemann, B. Vogel. Nucleation in the Karlsruhe plume during the COPS/TRACKS-Lagrange experiment. Quarterly Journal of the Royal Meteorological Society, 2011, 137, 267-274.

H. Junninen, A. Lauri, P. Keronen, P. Aalto, V. Hiltunen, P. Hari, M. Kulmala. Smart-SMEAR: on-line data exploration and visualization tool for SMEAR stations. Bor. Env. Res., 2009, 14, 447–457.

Keskinen, J., Pietarinen, K. and Lehtimäki, M.Electrical Low Pressure Impactor, J. Aerosol Sci., 1992, 23, 353-360.

W. Klug. A method for determining diffusion conditions from synoptic observations, Staub-Reinhalt. Luft, 1969 29, pp. 14-20.

C. Kuang, P. H. McMurry, A. V. McCormick, F. L. Eisele. 2008. Dependence of nucleation rates on sulphuric acid vapor concentration in diverse atmospheric locations. Journal of Geophysical Research, vol. 113, D10209, doi:10.1029/2007JD009253.

M. Kulmala, K.Lehtinen and A. Laaksonen. Cluster activation theory as an explanation of the linear dependence between formation rate of 3 nm particles and sulphuric acid concentration, Atmos. Chem. Phys., 2006, 6, pp. 787–793, doi:10.5194/acpd-6-787-2006.

S.W. Lee, T. Herage, R. Dureau, B. Young. Measurement of PM2.5 and ultra-fine particulate emissions from coal-fired utility boilers, Fuel, 2013, 108, 60-66.

K.E.J. Lehtinen, M. Dal Maso, M. Kulmala, V.-M. Kerminen. Estimating nucleation rates from apparent particle formation rates and vice versa: Revised formulation of the Kerminen-Kulmala equation. Journal of Aerosol Science, 2007, 38, 988–994.

Jos Lelieveld and Jost Heintzenberg. Sulfate Cooling Effect on Climate Through In-Cloud Oxidation of Anthropogenic SO_2. Science New Series, 1992, Vol. 258, No. 5079, Genome Issue (Oct. 2, 1992), 117-120

M. Levin, A. Gudmundsson, J. H. Pagels, M. Fiers, K. Mølhave, J. Löndahl, K. A. Jensen, I. K. Koponen. Limitations in the Use of Unipolar charging for Electrical Mobility Sizing Instruments: A Study of the Fast Mobility Particle Sizer. Aerosol Science and Technology, 2013, 49, 556-565.

C.R. Lonsdal, R.G. Stevens, C.A. Brock, P.A. Makar, E.M. Knipping, J.R. Pierce. The effect of coal-fired power plant SO2 and NOx control technologies on aerosol nucleation in the source plumes. Atmos. Chem. Phys., 2012, 12, 11519-11531.

Lähde, T., Rönkkö, Virtanen, A., Schuck, T.J., Pirjola, L., Hämeri, K, Kulmala, M., Arnold, F., Rothe, D., Keskinen, J. (2009) Heavy duty diesel engine exhaust aerosol particle and ion measurements. Environ. Sci. Technol., 2009, 43 (1), 163-168.

H. Marris, K. Deboudt, P. Augustin, P. Flament, F. Blond, E. Fiani, M. Fourmentin, H. Delbarre. Fast changes in chemical composition and size distribution of fine particles during the near-field transport of industrial plumes. Science of the total Environment, 2012, 427-428, 126-138.

Mikkanen, P., Moisio, M., Keskinen, J., Ristimäki, J., Marjamäki, M. Sampling method for particle measurements of vehicle exhaust. SAE Technical paper, 2001, 2001-01-0219.

S. Mikkonen, S. Romakkaniemi, J.N.Smith, H. Korhonen, T. Petäjä, C. Plass-Duelmer, M. Boy, P.H. McMurry, K.E.J. Lehtinen, J. Joutsensaari, A. Hamed, R.L. Mauldin III, W. Birmili, G. Spindler, F. Arnold, M. Kulmala,

A. Laaksonen. A statistical proxy for sulphuric acid concentration, Atmos. Chem. Phys., 2011, 11, 11319-11334.

Mirme, A.. Electric aerosol spectrometry. Ph. D. Thesis, Tartu University, 1994.

F. Pasquill, The estimation of the dispersion of windborne material, The Meteorological Magazine, 1961, 90 (1063), pp 33-49.

Pearson, G., Davies, F., Collier, C. An analysis of the Performance of the UFAM Pulsed Doppler Lidar for observing the Boundary Layer. J. Atmos. Ocean. Tech., 2009, 26, 240–250, doi:10.1175/2008JTECHA1128.1.

Petäjä, T., Mauldin, III, R. L., Kosciuch, E., McGrath, J., Nieminen, T., Paasonen, P., Boy, M., Adamov, A., Kotiaho, T., and Kulmala, M.: Sulfuric acid and OH concentrations in a boreal forest site, Atmos. Chem. Phys., 9, 7435-7448, doi:10.5194/acp-9-7435-2009, 2009.

L. Pirjola, A. Pajunoja, J. Walden, J.-P. Jalkanen, T. Rönkkö, A. Kousa, T. Koskentalo 2014 Mobile measurements of shi emissions in two harbour areas in Finland, Atmos. Measu. Tech., vol 7, pp. 149-161.

L. Pirjola, M. Karl, T. Rönkkö, and F. Arnold. Model studies of volatile diesel exhaust particle formation: are organic vapours involved in nucleation and growth?, Atmospheric Chemistry and Physics, 2015, 13, 10435-10452.

J. Ristimäki, A. Virtanen , M. Marjamäki, A. Rostedt, J. Keskinen. 2002. On-line measurement of size distribution and effective density of submicron aerosol particles; Journal of Aerosol Science, vol 33, num 11, pp. 1541-1557

T. Rönkkö, A. Arffman, P. Karjalainen, T. Lähde, J. Heikkilä, L. Pirjola, D.Rothe, J.Keskinen. Diesel exhaust nanoparticle volatility studies by a new thermodenuder with low solid nanoparticle losses, ETH Conference on Combustion Generated Nanoparticles, 2011.

Saari, S., Karjalainen, P., Ntziachristos, L., Pirjola, L., Matilainen, P., Keskinen, J., Rönkkö, T. (2016) Exhaust particle and NO_x emission performance of an SCR heavy duty truck operating in real-world conditions. Atmospheric Environment, 126, pp. 136–144, 10.1016/j.atmosenv.2015.11.047

K. Saarnio, A. Frey, J.V. Niemi, H. Timonen, T. Rönkkö, P. Karjalainen, M. Vestenius, K. Teinilä, L. Pirjola, V. Niemelä, J. Keskinen, A. Häyrinen, R. Hillamo. 2014 Chemical composition and size of particles in emissions of coal-fired power plant with flue gas desulphurization, Journal of Aerosol Science, vol 73, 14-26.

N. Sarnela, T. Jokinen, T. Nieminen, K. Lehtipalo, H. Junninen, J. Kangasluoma, J. Hakala, R. Taipale, S. Schobesberger, M. Sipilä, K. Larnimaa, H. Westerholm, J. heijari, V.-M. Kerminen, T. Petäjä, M. Kulmala. 2015. Sulphuric acid and aerosol particle production in the vicinity of an oil refinery. Atmospheric Environment, 119, pp. 156–166.

J. H. Seinfeld, S.N. Pandis. Atmospheric chemistry and physics: from air pollution to climate change, second edition. John Wiley & Sons Inc., New York, 2006.

S.-L. Sihto, M. Kulmala, V.-M. Kerminen, M. Dal Maso, T. Petäjä, I. Riipinen, H. Korhonen, F. Arnold, R. Janson, M. Boy, A. Laaksonen, K. E. J. Lehtinen (2006) Atmospheric sulphuric acid and aerosol formation: implications from atmospheric measurements for nucleation and early growth mechanisms. Atmospheric Chemistry & Physics, 6, pp. 4079-4091.

R. K. Srivastava & W. Jozewicz (2001) Flue Gas Desulfurization: The State of the Art, Journal of the Air & Waste Management Association, 51:12, 1676-1688

R. G. Stevens and J. R. Pierce. A parameterization of sub-grid particle formation in sulfur-rich plumes for global- and regional-scale models, Atmos. Chem. Phys., 2013, 13, 12117-12133.

R.G. Stevens, J.R. Pierce, C.A. Brock, M.K. Reed, J.H. Crawford, J.S. Holloway, T.B. Ryerson, L.G. Huey, J.B. Nowak. Nucleation and growth of Sulfate aerosol in coal-fired power plant plumes: sensitivity to background aerosol and meteorology. Atmos. Chem. Phys., 2012, 12, 189-206

J. M. Stockie. The Mathematics of Atmospheric Dispersion Modeling, SIAM Review, 2011, Vol. 53, No. 2, pp. 349–372.

Stolzenburg, M. R., P. H. McMurry, H. Sakurai, J. N. Smith, R. L. Mauldin III, F. L. Eisele, and C. F. Clement. Growth rates of freshly nucleated atmospheric particles in Atlanta, J. Geophys. Res., 2005, 110, D22S05, doi:10.1029/2005JD005935.

Wang, S. C., Flagan, R. C. Scanning Electrical Mobility Spectrometer. Aerosol Science and Technology, 1990, (13), 230–240.

H. Yi, J. Hao, L. Duan, X. Tang, P. Ning, X. Li. Fine particle and trace element emissions from an anthracite coal-fired power equipped with bag-house in China, Fuel, 2008, 87, 2050-2057.